# Development of Selective Axonopathy in Adult Sensory Neurons Isolated From Diabetic Rats
## Role of Glucose-Induced Oxidative Stress

Elena Zherebitskaya,[1] Eli Akude,[1,2] Darrell R. Smith,[1,2] and Paul Fernyhough[1,2]

**OBJECTIVE**—Reactive oxygen species (ROS) are pro-oxidant factors in distal neurodegeneration in diabetes. We tested the hypothesis that sensory neurons exposed to type 1 diabetes would exhibit enhanced ROS and oxidative stress and determined whether this stress was associated with abnormal axon outgrowth.

**RESEARCH DESIGN AND METHODS**—Lumbar dorsal root ganglia sensory neurons from normal or 3- to 5-month streptozotocin (STZ)-diabetic rats were cultured with 10 or 25–50 mmol/l glucose. Cell survival and axon outgrowth were assessed. ROS were analyzed using confocal microscopy. Immunofluorescent staining detected expression of manganese superoxide dismutase (MnSOD) and adducts of 4-hydroxy-2-nonenal (4-HNE), and MitoFluor Green dye detected mitochondria.

**RESULTS**—Dorsal root ganglion neurons from normal rats exposed to 25–50 mmol/l glucose did not exhibit oxidative stress or cell death. Cultures from diabetic rats exhibited a twofold ($P < 0.001$) elevation of ROS in axons after 24 h in 25 mmol/l glucose compared with 10 mmol/l glucose or mannitol. Perikarya exhibited no change in ROS levels. Axonal outgrowth was reduced by approximately twofold ($P < 0.001$) in diabetic cultures compared with control, as was expression of MnSOD. The antioxidant N-acetyl-cysteine (1 mmol/l) lowered axonal ROS levels, normalized aberrant axonal structure, and prevented deficits in axonal outgrowth in diabetic neurons ($P < 0.05$).

**CONCLUSIONS**—Dorsal root ganglia neurons with a history of diabetes expressed low MnSOD and high ROS in axons. Oxidative stress was initiated by high glucose concentration in neurons with an STZ-induced diabetic phenotype. Induction of ROS was associated with impaired axonal outgrowth and aberrant dystrophic structures that may precede or predispose the axon to degeneration and dissolution in human diabetic neuropathy. *Diabetes* 58:1356–1364, 2009

Diabetic sensory polyneuropathy in humans and animal models is associated with a spectrum of structural changes in peripheral nerves that includes microangiopathy, axonal degeneration, segmental demyelination, and ultimately loss of both myelinated and unmyelinated fibers (1,2). It has been proposed that high glucose concentrations induce toxicity and cell death in sensory neurons, and this triggers diabetic neuropathy through loss of nerve fibers (3). Cultured embryonic dorsal root ganglion sensory neurons were exposed to high nonphysiological concentrations of glucose that induced oxidative stress by increasing production of reactive oxygen species (ROS), and this was associated with mitochondrial dysfunction, which resulted in programmed cell death (4–6).

Morphologic studies have provided a variety of results in relation to sensory neuron survival in animal models of diabetes. Long-term studies of 9 months in streptozotocin (STZ)-diabetic mice revealed a significant loss of sensory neurons (7). In STZ-diabetic rats of up to 12 months' duration, no significant loss of adult lumbar dorsal root ganglion neurons was observed (8,9). Additionally, in 4-month diabetic BB rats, there was no dorsal root ganglion sensory neuron cell death (10); however, by 10 months there was progressive neuronal loss, but prominent only in the small dorsal root ganglion neuron population and not involving apoptosis (11). At the same time there was a significant decrease in the numbers of myelinated and unmyelinated fibers, but no evidence of structural changes in mitochondria in dorsal root ganglion sensory neurons (11). In STZ-diabetic mice, where loss of small neurons was also occurring, there was no sign of activation of the pro-apoptotic markers p38, caspase-3, and phosphorylated c-jun (12).

Sural nerves from humans with diabetic neuropathy assessed using quantitative morphometry have significant endoneurial microangiopathy, early structural abnormalities in Schwann cells in myelinated fibers, and degeneration and loss of unmyelinated and myelinated fibers; however, in intact axons, mitochondria appeared structurally normal (1,13). In addition, studies performed on postmortem samples from type 2 diabetic patients have shown the occurrence of dystrophic changes in axon terminals and within the dorsal root ganglion and autonomic ganglia, but no evidence for significant neuronal cell loss (14,15).

These results show that in vivo in animals and humans, the impact of diabetes on sensory neuron survival are discordant with the in vitro studies demonstrating toxic effects of high glucose concentration leading to apoptosis.

We hypothesized that the underlying reason for this discrepancy was the use of embryonic sensory neurons for in vitro glucose toxicity studies (3). Cultured embryonic sensory neurons have phenotypic differences with adult sensory neurons and are dependent on neurotrophic factor–derived support for survival (16). Therefore, the aim of this study was to compare responses of adult dorsal root ganglion sensory neurons from age-matched control and 3- to 5-month STZ-diabetic rats exposed to high glucose concentration. To this end, the effect of high glucose concentration on oxidative stress and neuronal survival and axonal morphology was assessed.

## RESEARCH DESIGN AND METHODS

Dorsal root ganglion sensory neurons from adult Sprague-Dawley male rats were isolated and dissociated using a previously described method (17–19). Rats were age-matched control or 3- to 5-month STZ-diabetic rats that included cohorts receiving insulin implants (two Linplant implants placed subcutaneously; LinShin Canada, North Scarborough, ON, Canada). Rats were made diabetic with a single intraperitoneal injection of 75 mg/kg STZ (Sigma, St. Louis, MO). End points for body weight, plasma glucose, and hemoglobin A1C are presented in supplementary Table 1, which is available in an online appendix at http://diabetes.diabetesjournals.org/cgi/content/full/db09-0034/DC1. Cells were plated onto poly-DL-ornithine and laminin-coated 12-well plates (Nunclon Surface, Ottawa, ON, Canada) for the neuronal survival study, 25-mm glass cover slips (German glass no. 1; Electron Microscopy Sciences, Hatfield, PA) for neurite outgrowth and for immunocytochemistry, and 35-mm glass-bottom dishes for ROS measurement (catalog no. W20; Bioscience Tools, San Diego, CA). Neurons were cultured in Ham's F12 medium (Invitrogen, Carlsbad, CA) with 10% fetal bovine serum (FBS; HyClone, Logan, UT) for long-term cultures (>5 days). For short-term cultures, neurons were grown in defined medium with modified Bottenstein and Sato's N2 medium containing: 0.1 mg/ml transferrin, 20 nmol/l progesterone, 100 µmol/l putrescine, 30 nmol/l sodium selenite, and 10 mg/ml BSA (the modified N2 formulation used did not include insulin; all obtained from Sigma). Neuronal survival was quantified by established methods (20,21). Viable neurons were counted before experimental treatment and at time points after treatment. Neurons that died in the intervals between examination points were absent, and the viability of the remaining neurons was assessed by morphologic criteria. Neurons with membranes and soma with a smooth round appearance were viable, whereas neurons with fragmented or distended membranes and vacuolated soma were nonviable. Four images were collected from each well and from the same place using marked grids on each well bottom at 1, 4, 7, 21, and 28 days using a light microscope (phase contrast Nikon Diaphot). Survival was confirmed by trypan blue exclusion at the last time point. For neurite outgrowth measurements, images of cultures were collected from 10 random fields from each well. The longest axon and total number of neurons and number of intersects of their neurites with a vertical grid were counted using a morphometric approach and SigmaScan Microsoft software. The total number of intersects per neuron was taken as the parameter of total axon outgrowth as previously described (22).

**ROS measurement.** ROS levels were detected using real-time fluorescence microscopy on a Carl Zeiss LSM510 inverted confocal microscope using two dye-based approaches: *1*) dihydrorhodamine 123 (DHR123) and *2*) 5-(and-6)-chloromethyl-2′7′-dichlorodihydrofluorescein diacetate acetyl ester (CM-H$_2$DCFDA). Neurons were loaded with 5 µmol/l of DHR123 (in 100% EtOH; Sigma) or 1.2 µmol/l CM-H$_2$DCFDA (in 100% anhydrous DMSO; Molecular Probes) for 30 or 15 min, respectively, at 37°C, and then washed three times with F-12 and visualized using the argon laser (at 2% power). For DHR123, excitation (max) was 505 nm and emission (max) 534 nm, and for CM-H$_2$DCFDA, excitation (max) was 488 nm and emission collected above 510 nm. Images were collected and analyzed as pixel intensity at the level of the axon or cell body. For axonal signals, all axons in each field were assessed, and, using the Carl Zeiss software package, a line was placed along the length of the axon and pixel intensity collected per micrometer of axon. Control experiments were performed to confirm that the DHR123 and CM-H$_2$DCFDA signals were sensitive to antioxidant (N-acetyl-cysteine) or pro-oxidant (H$_2$O$_2$) treatment (not shown).

**Immunocytochemistry for activated caspase 3,4-hydroxy-2-nonenal, manganese superoxide dismutase, and phosphorylated neurofilament H.** Dorsal root ganglion neurons were fixed with 4% paraformaldehyde in phosphate buffer at pH 7.4 for 15 min followed by permeabilizing with 0.3% Triton X-100 in PBS. Nonspecific binding was blocked by incubation with blocking reagent combined with FBS and 1.0 mol/l PBS in proportions of 3:1:1

(catalog no. 1 096 176; Roche, Indianapolis, IN) for 1 h at room temperature and washed with PBS three times. Cells were then incubated with antibodies to β-tubulin isotype III (1:1,000; Sigma, Oakville, ON, Canada), caspase 3 (1:100; Chemicon, Temecula, CA), (E)-4-hydroxy-2-nonenal (4-HNE) adducts (1:500 anti-4-HNE adducts Pab; Alexis Biochemicals, San Diego, CA), manganese superoxide dismutase (MnSOD; 1:300; StressGen, Ann Arbor, MI), and phosphorylated neurofilament H (NFH; 1:500 SMI-31; Covance, Berkeley, CA). For localization of mitochondria, live cultures of dorsal root ganglion neurons were treated for 15 min with 200 nmol/l MitoFluor Green dye (Molecular Probes, Eugene, OR) before being fixed for immunostaining for anti-NFH. Primary antibodies were incubated with slides overnight in a humidified chamber followed by fluorescein isothiocyanate– and CY3-conjugated secondary antibodies (Jackson ImmunoResearch Laboratories, West Grove, PA; 1:250) for 3 h at room temperature. Fluorescence signals were examined and quantified using a Carl Zeiss Axioscop-2 mot microscope with AxioVision 3 software and equipped with fluorescein isothiocyanate, CY3, 4′,6-diamidino-2-phenylindole filters, and an AxioCam camera.

**Data analysis.** Because of the technically difficult nature of the cultures and the image acquisition, not all images were collected in a blinded fashion, although a random approach was taken for image capture from each well. Where appropriate, data were subjected to one-way ANOVA with post hoc comparison using Tukey's test (Prism 4; GraphPad Software, San Diego, CA). In all other cases, standard two-tailed unpaired Student's $t$ test with Welch's correction was performed, which does not assume equal variances, with significance levels of $P = 0.05$, using GraphPad Prism 4.

## RESULTS

Initial experiments were designed to test the influence of high concentrations of glucose (50 mmol/l) on survival of sensory neurons in culture, the induction of apoptosis, and markers of oxidative stress. Sensory neurons from adult control rats were grown up to 4 weeks in F12 medium with 10% FBS. Healthy neurons were phase bright, and by 1 week, cultures exhibited high numbers of nonneuronal cells, including Schwann cells, satellite cells, and fibroblasts (Fig. 1A and B). High glucose concentration had no effect on survival of neurons at any time and did not affect axon outgrowth on day 1 (Fig. 1C and *insert*). Surviving dorsal root ganglion neurons did decline over time and had diminished by 50% by the 28th day; however, there was no effect of 50 mmol/l glucose on this process. Oxidative stress and/or induction of apoptosis was assessed by staining for adducts of 4-HNE and caspase 3 activation. There was no effect of 50 mmol/l glucose on caspase 3 or 4-HNE adduct expression in neuronal perikarya at 2 or 4 weeks (Fig. 1D and E). However, there was a small (10–20%), but statistically significant, increase of activation of caspase 3 and 4-HNE adduct expression in the 4- vs. 2-week group of dorsal root ganglion neurons; this effect was not perturbed by 50 mmol/l glucose.

A second set of experiments tested whether high glucose concentration induced oxidative stress in neuronal perikarya or axons in cultures of adult sensory neurons under defined conditions in F12 + modified N$_2$ medium. To assess oxidative stress, a real-time video microscopy approach was taken using the fluorescent dye CM-H$_2$DCFDA. This dye is believed to give a readout of cellular ROS levels, including peroxynitrite, hydrogen peroxide, and hydroxyl radicals. Neurons were grown 24 h under control (10 mmol/l glucose) or high (25 mmol/l) glucose. Supplementary Fig. 1 shows no effect of 25 mmol/l glucose on CM-H$_2$DCFDA intensity in neuronal perikarya (supplementary Fig. 1A) or axons (supplementary Fig. 1B). High glucose concentration did not elevate 4-HNE adducts in cell bodies (supplementary Fig. 1C) or axons (supplementary Fig. 1D).

We next determined whether cultured neurons from STZ-diabetic rats were also refractory to high glucose concentration. Neurons from age-matched control rats
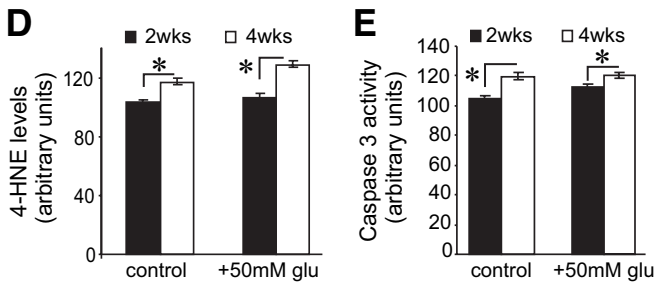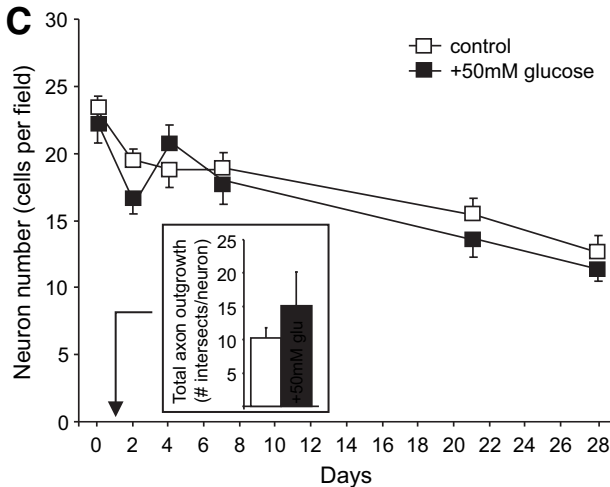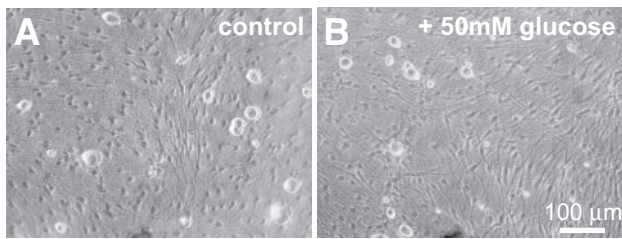
FIG. 1. High glucose concentration does not impair adult sensory neuron survival or induce oxidative stress. *A* and *B*: Phase contrast images of 2-week cultures of adult dorsal root ganglion sensory neurons grown in defined F12 + 10% FBS medium with and without 50 mmol/l D-glucose. Note the phase-bright neuronal perikarya and phase-dark nonneuronal cells (mostly fibroblasts and Schwann cells). *C*: Levels of survival of dorsal root ganglion neurons for control (10 mmol/l D-glucose) or 50 mmol/l D-glucose over a 4-week period. Cell numbers were assessed by morphology under a phase contrast microscope. Values are the means ± SE, $n = 4$ replicate cultures. The insert graph shows no difference in total axonal outgrowth at 24 h. Values are the means ± SE, $n = 3$ replicate cultures. *D* and *E*: Levels of 4-HNE adduct expression or caspase 3 activation in neuronal perikarya in arbitrary units of fluorescence intensity at 2 and 4 weeks of culture. Values are the means ± SE, $n = 85–108$ neurons. *$P < 0.05$. glu, glucose; wks, weeks.

were grown in defined F12 + modified $N_2$ medium under low (10 mmol/l) glucose with 10 nmol/l insulin, whereas neurons from 3- to 4-month STZ-diabetic rats were grown in F12 + modified $N_2$ medium with 25 mmol/l glucose with no insulin support (to attempt to mimic diabetes in vivo). Cell survival of neurons from normal and diabetic rats over a 4-day period and under defined conditions were identical. Figure 2 shows the phase contrast images of sensory neurons from control (Fig. 2*A*, *upper* and *lower panels*) and STZ-diabetic (Fig. 2*B*) rats after 4 days in culture. Diabetic dorsal root ganglion neurons exhibited abnormal morphologic changes in neurite outgrowth, which were characterized by less axonal outgrowth (Fig. 2*C*) and appearance of phase-dark axonal swellings and
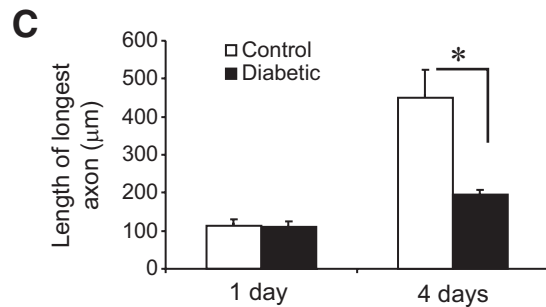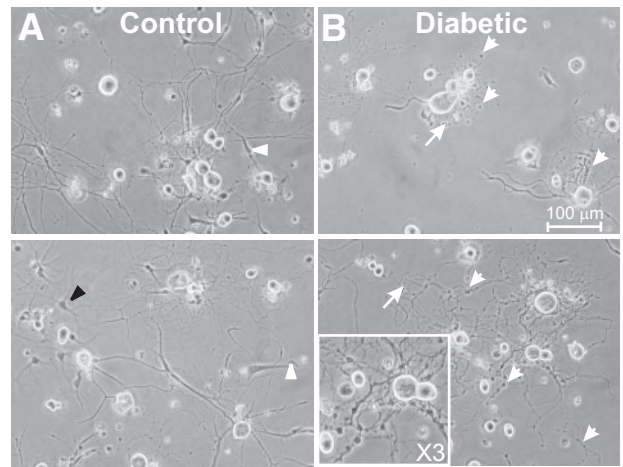


FIG. 2. Cultured sensory neurons from STZ-diabetic rats exhibit abnormal morphology and reduced levels of axon outgrowth. *A*: Upper and lower panels show phase contrast images of neurons derived from normal rats at 4 days in culture in defined F12 + modified $N_2$ medium with 10 nmol/l insulin. *B*: Upper and lower panels show images of cultures derived from 3- to 4-month STZ-diabetic rats and grown in defined media with 25 mmol/l glucose and no insulin. White arrows show areas of abnormal axonal structure highlighted by swelling and beading. The insert shows a ×3 image exhibiting the phase-dark axonal swellings. White arrowheads are rare swellings in normal neurons. Black arrowheads are nonneurons. *C*: Quantification of axonal outgrowth, longest axon, after 1 and 4 days of culture from control or STZ-diabetic rats. Values are the means ± SE, $n = 58–97$ axons. *$P < 0.001$.

beading along neurites (Fig. 2*B*, *lower panel, inset*). Separate cultures from control or STZ-diabetic rats were grown for 1 day and assessed for level of ROS in cell bodies and axons using CM-$H_2$DCFDA (Fig. 3*A*, *B*, and *E*) or DHR123 (Fig. 3*C*, *D*, and *F*) fluorescence imaging. ROS levels in cell bodies did not differ between control and diabetic neurons (not shown). Axonal ROS levels in neurons from STZ-diabetic rats showed at least a twofold elevation compared with control using both dyes (Fig. 3*E* and *F*). Cultures were then grown for 4 days and immunostained for 4-HNE adducts and β-tubulin III. Control cultures exhibited normal axons with very rare instances of axonal swellings (or varicosities); such swellings were negative for 4-HNE adduct staining (Fig. 4*A*, *C*, and *E*). In comparison, cultures from STZ-diabetic rats demonstrated large numbers of axonal swellings that were characterized with positive staining for 4-HNE adducts (Fig. 4*B*, *D*, and *F*). The cell bodies of control and diabetic cultures revealed similar levels of highly positive staining for 4-HNE adducts.

It was important to determine whether differences in axonal morphology, ROS levels, and 4-HNE staining between control and diabetic cultures was controlled by acute effects in the culture of glucose concentration and/or insulin. Dorsal root ganglion sensory neurons from STZ-
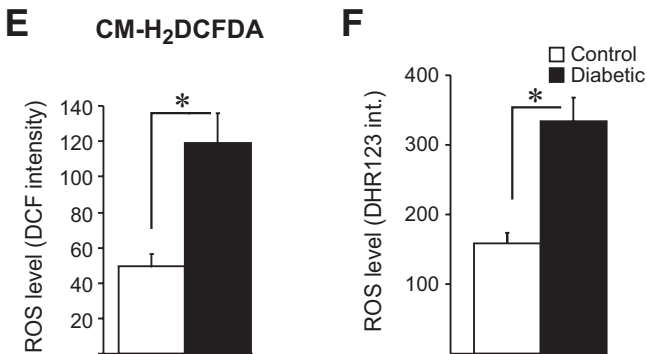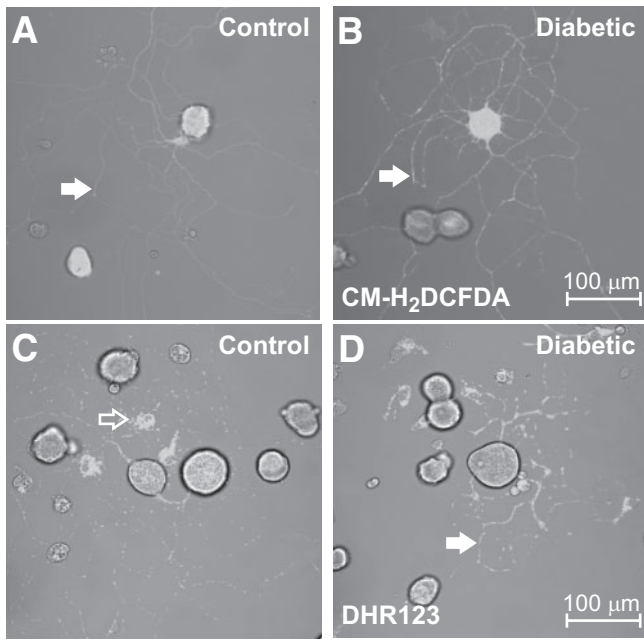
**FIG. 3. Axons of sensory neurons from STZ-diabetic rats exhibit elevated level of ROS.** *A* and *C*: Images of ROS levels in axons at 24 h of adult dorsal root ganglion neuron culture from control rats. Cultures were stained for ROS using CM-H$_2$DCFDA (*A*) or DHR123 (*C*) dye, and cells were grown in defined F12 + modified N$_2$ medium with 10 nmol/l insulin. *B* and *D*: Axonal ROS level at 24 h of adult dorsal root ganglion neuron culture from 3- to 4-month STZ-diabetic rats. Cells were grown in defined F12 + N$_2$ medium with 25 mmol/l glucose and without insulin. Solid arrows show axons that were quantified for ROS level. Open arrow indicates a nonneuronal source of ROS. *E* and *F*: Quantification of ROS accumulation in axons of dorsal root ganglion neurons from control and STZ-diabetic rats is shown in a bar graph derived from CM-H$_2$DCFDA (*E*) or DHR123 (*F*) staining. Values are the means ± SE, n = 55–64 axons. *$P < 0.001$. int., intensity.



**FIG. 4. Axons of neurons of STZ-diabetic rats exhibit swellings that include adducts of 4-HNE.** *A*, *C*, and *E*: Merged immunofluorescent images stained for 4-HNE (green) and neuron-specific β-tubulin III (orange) at 4 days of sensory neuron culture from control rats (blue nuclei were stained with 4′,6-diamidino-2-phenylindole). Cells were grown in F12 + modified N$_2$ defined medium with 10 mmol/l D-glucose and with 10 nmol/l insulin. *B*, *D*, and *F*: Merged immunofluorescent images of cultures from STZ-diabetic rats grown in F12 + modified N$_2$ defined medium with 25 mmol/l D-glucose and without insulin. White arrows show 4-HNE adduct accumulation in axon swellings in STZ-diabetic neurons. Red arrows show β-tubulin III accumulation in rare swellings without 4-HNE. Yellow arrows indicate nonneurons. Asterisks indicates perikarya strongly labeled for 4-HNE. (A high-quality digital representation of this figure is available in the online issue.)

diabetic rats were cultured at 10 mmol/l glucose, 25 mmol/l glucose, and 15 mmol/l mannitol (+ 10 mmol/l glucose) in defined F12 + modified N$_2$ medium without insulin support. ROS level in axons was measured after 1 day of culture (Fig. 5*A* and *B*). Quantification of ROS accumulation in axons using CM-H$_2$DCFDA dye showed a statistical increase in ROS levels after high glucose administration compared with low glucose concentration (Fig. 5*E*). High mannitol concentration revealed an intermediate level of ROS production in axons (Fig. 5*E*). 4-HNE adduct accumulation in axons of sensory neurons from STZ-diabetic rats was measured after 3 days of culture (Fig. 5*C* and *D*). High glucose concentration induced a significant increase in 4-HNE adduct accumulation in axons compared with those cultured at 10 mmol/l glucose and mannitol (Fig. 5*F*). Neurons isolated from STZ-diabetic rats treated for the final month with insulin that
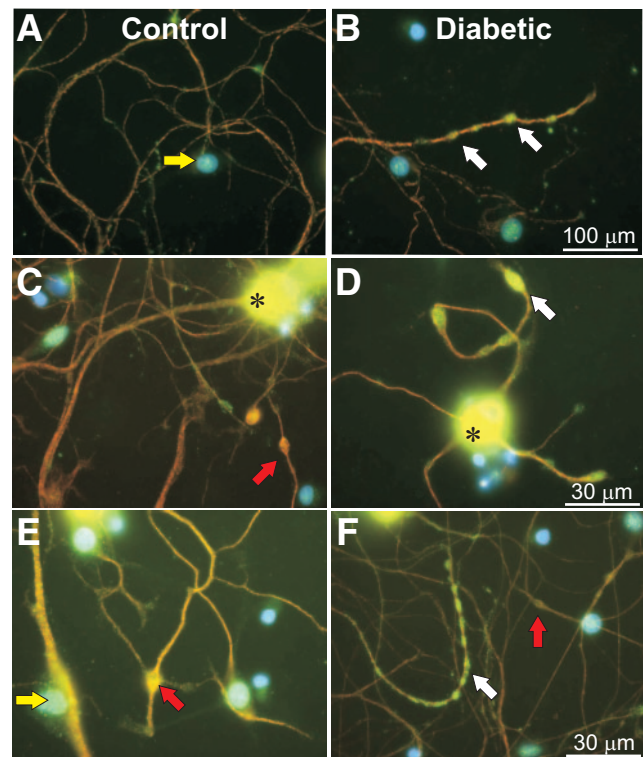
significantly lowered hyperglycemia (supplementary Table 1) did not respond to high glucose with elevated ROS or 4-HNE accumulation in axons (Fig. 5*E* and *F*). Studies were also performed in which STZ-diabetic neurons were treated with 10 nmol/l insulin in the presence of low or high glucose concentration, and under such conditions there was no impact on ROS or 4-HNE levels of the insulin treatment (data not shown). In addition, an alternative control was used for mannitol, 15 mmol/l L-glucose, and results were the same as those seen with mannitol.

Experiments now determined whether oxidative stress was causally linked to aberrant axonal structure in neurons derived from STZ-diabetic rats. The antioxidant N-acetyl cysteine (NAC) was tested for its ability to lower ROS. Cultures from control rats were assessed for ROS using DHR123 imaging and treated acutely with 1 mmol/l NAC (Fig. 6). Figure 6*A–D* shows that NAC rapidly neutralized ROS levels. In a separate experiment, STZ-diabetic cultures were plated for 1 day in the presence or absence of 1 mmol/l NAC, and effect on axonal outgrowth was determined; NAC was clearly able to enhance levels of total axonal outgrowth (Fig. 6*E*). Cultures of sensory neurons from control or STZ-diabetic rats were maintained for 3 days (at this time point, diabetic neurons exhibited 4-HNE staining) (Fig. 5*C* and *D*). During the last 24 h of culture, control and STZ-diabetic neurons were
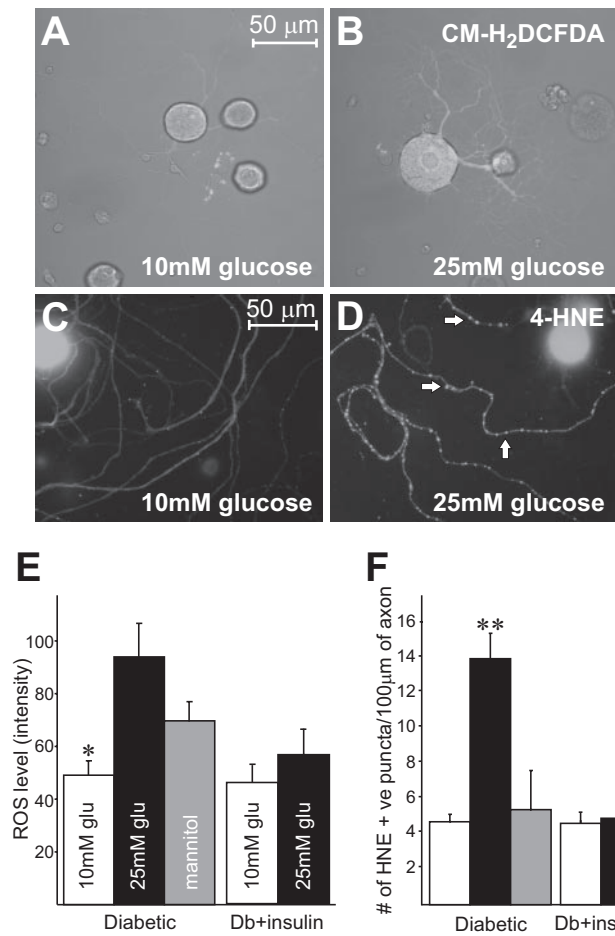
FIG. 5. High glucose concentration elevates ROS and adducts of 4-HNE in axons of sensory neurons from STZ-diabetic rats. *A* and *B*: Images of sensory neuron cultures, which were assessed for ROS in axons on day 1 using CM-H$_2$DCFDA at 10 mmol/l D-glucose (*A*) or 25 mmol/l D-glucose (*B*) or 15 mmol/l D-mannitol (with 10 mmol/l glucose; image not shown) in defined F12 + modified N$_2$ medium. *E*: Quantification of ROS accumulation in axons of dorsal root ganglion cultures from control, diabetic, or diabetic treated with insulin animals using CM-H$_2$DCFDA emission. Values are the means ± SE, $n$ = 44–57 axons. *$P$ < 0.05 vs. 25 mmol/l glucose. *C* and *D*: Immunofluorescent images of accumulation of adducts of 4-HNE in axons in sensory neuron cultures after 3 days in defined F12 + N$_2$ medium with 10 mmol/l D-glucose (*C*) or 25 mmol/l D-glucose (*D*) (individual puncta are indicated by white arrows; 15 mmol/l mannitol; image not shown). *F*: Levels of accumulation of puncta of adducts of 4-HNE in axons. Values are the means ± SE, $n$ = 3–6 replicate cultures. **$P$ < 0.05 vs. other groups (one-way ANOVA with Tukey's post hoc comparison). □, 10 mmol/l glucose; ■, 25 mmol/l glucose; ▨, mannitol. Db, diabetic; +ve, positive.

treated with 1 mmol/l NAC for a further 24 h. After 4 days all groups of cultures were treated with MitoFluor Green dye to specifically stain mitochondria and then fixed and immunostained for phosphorylated NFH. Figure 7*A* and *B* shows control neurons with normal axonal structure and uniform axonal localization of mitochondria. Cultures from STZ-diabetic rats demonstrated abnormal accumulations of mitochondria in axons that colocalized with phosphorylated NFH staining (Fig. 7*C* and *D*). Treatment with 1 mmol/l NAC significantly lowered the number of axonal swellings in normal and STZ-diabetic cultures (Fig. 7*E–G*).

Increased ROS under high glucose concentration in diabetic neurons may reflect an impaired capacity to scavenge free radicals. Therefore, the effect of diabetes and high glucose on the expression of MnSOD was assessed in isolated mitochondrial preparations from dorsal
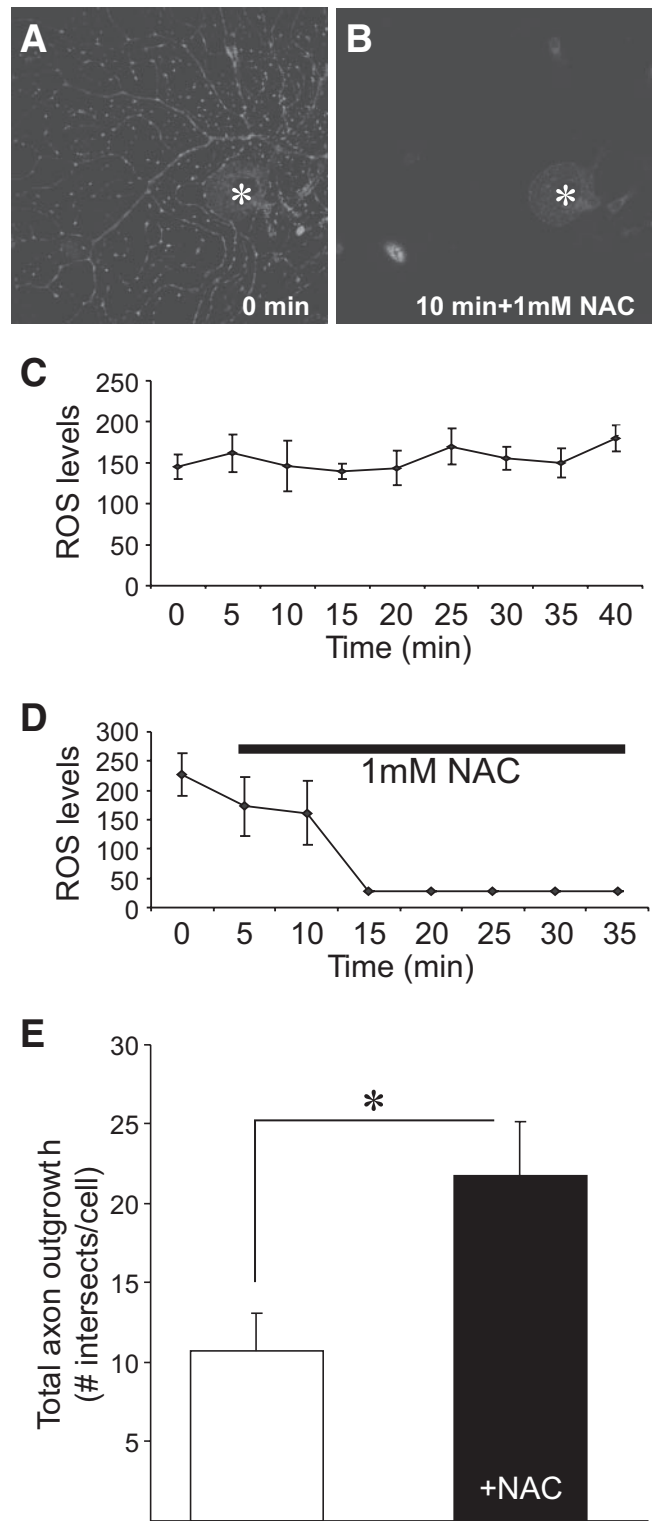


FIG. 6. Treatment with antioxidant NAC lowers ROS levels in axons and elevates axon outgrowth. ROS levels, measured using DHR123, in axons before (*A*) and after (*B*) 10 min of treatment with 1 mmol/l NAC (asterisk indicates perikarya of neuron). *C* and *D*: Real-time imaging data of ROS levels in axons before (*C*) and after (*D*) 1 mmol/l NAC treatment. Values are the means ± SE, $n$ = 4–6 axons. *E*: Total axon outgrowth for STZ-diabetic neurons cultured for 24 h with (■) or without (□) 1 mmol/l NAC. Values are the means ± SE, $n$ = 3 replicate cultures. *$P$ < 0.05.

root ganglia and in cultured sensory neurons. In Fig. 8, we present Western blot data demonstrating that MnSOD expression was reduced by 32% ($P$ < 0.005) in mitochon-
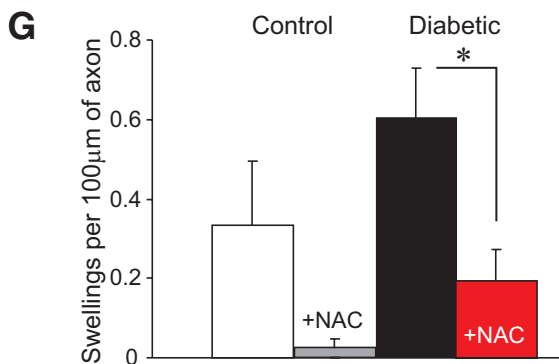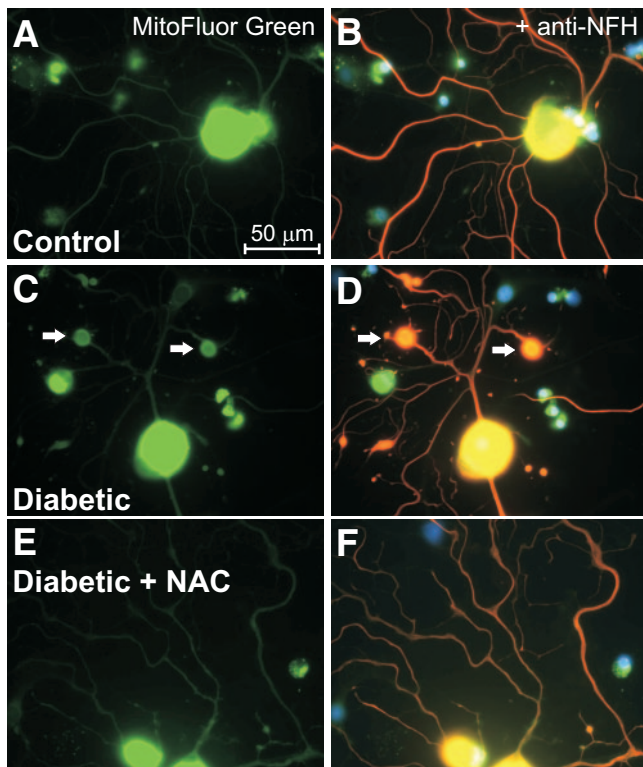
FIG. 7. Axonal swellings in neurons from STZ-diabetic rats exposed to high glucose represent accumulations of mitochondria and phosphorylated NFH, which are eliminated by antioxidant treatment. In the left column of immunofluorescent images is MitoFluor Green staining; the right column exhibits phosphorylated NFH staining (orange). Double-staining is yellow. Dorsal root ganglion sensory neuron cultures were derived from age-matched control or 3- to 4-month STZ-diabetic rats and maintained in defined media for 4 days. STZ-diabetic rat cultures were grown in 25 mmol/l glucose without insulin. During the final 24 h of culture time, selected control or diabetic cultures were treated with 1 mmol/l NAC. A–F: Control (A and B), STZ-diabetic (C and D), and STZ-diabetic culture treated for 24 h with 1 mmol/l NAC (E and F). White arrows indicate areas of colocalization of mitochondria and phosphorylated NFH. G: Quantification of the number of axonal swellings in each treatment group. Values are the means ± SE, n = 3 replicate cultures. *P < 0.05. (A high-quality digital representation of this figure is available in the online issue.)
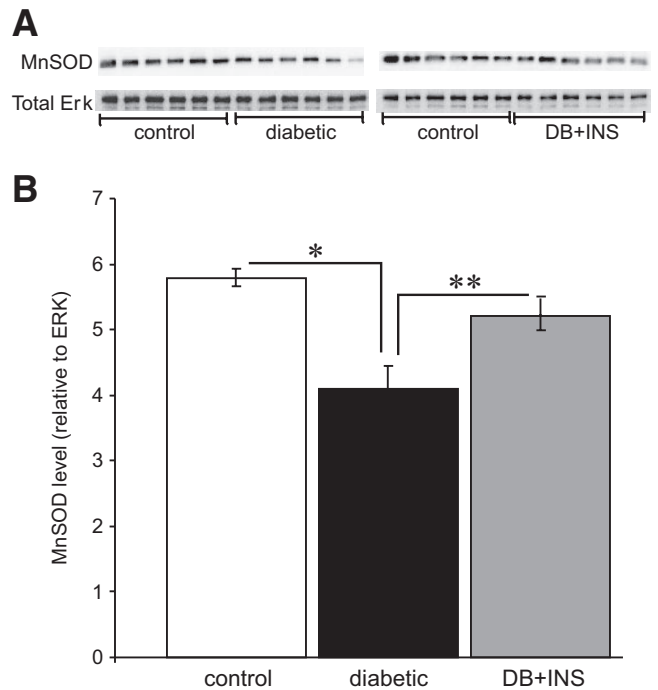


FIG. 8. MnSOD expression is reduced in mitochondria of dorsal root ganglion from STZ-diabetic rats. Dorsal root ganglia from 5-month control, STZ-diabetic, or insulin-treated diabetic rats were homogenized in mitochondrial isolation buffer containing: 10 mmol/l HEPES (pH 7.4), 200 mmol/l mannitol, 70 mmol/l sucrose, and 1 mmol/l EGTA. The dorsal root ganglion homogenate was centrifuged at 800$g$ for 10 min at 4°C followed by centrifugation of the supernatant at 8,000$g$ for 15 min, and the mitochondrial pellet was collected. Mitochondrial protein preparations (5 μg/lane) were resolved on a 12% SDS-PAGE gel and electroblotted (30V, 16 h) onto nitrocellulose membrane. Blots were then blocked in 5% nonfat milk containing 0.05% Tween overnight at 4°C, rinsed in PBS (pH 7.4), and then incubated with rabbit anti-MnSOD polyclonal antibody (1:2,000 dilution) overnight at 4°C. Extracellular signal–regulated kinase (1:2,000; Covance) was probed as a loading control (previously shown not to change in diabetes in dorsal root ganglia). The blots were rinsed, incubated in Super Signal West Pico (Pierce Biotechnology, Rockford, IL), and imaged using a BioRad Fluor-S image analyzer. A and B: Shown are the blots (A) and chart (B) in which MnSOD signal has been presented relative to total extracellular signal–regulated kinase levels. Values are the means ± SE, n = 6. *P < 0.005 vs. control; **P = 0.056 vs. diabetic + insulin (one-way ANOVA with Tukey's test). DB, diabetic; Erk and ERK, extracellular signal–regulated kinase; INS, insulin.

dria isolated from dorsal root ganglia of STZ-diabetic rats, and this was prevented by insulin therapy. Figure 9A and B shows axonal staining of MnSOD in sensory neurons from age-matched control rats cultured for 1 day under 10 mmol/l glucose. Results were similar under 25 mmol/l glucose (images not shown). Neurons from STZ-diabetic rats cultured under 10 mmol/l glucose for 1 day exhibited diminished immunostaining for MnSOD (Fig. 9C and D); however, if cultured in the presence of 25 mmol/l glucose, then no alteration in MnSOD expression was observed (Fig. 9E and F). When cultures were maintained for 3 days in vitro, the ability of 25 mmol/l glucose to maintain or raise MnSOD expression was significantly impaired (Fig. 9G and H).

## DISCUSSION

This work demonstrates for the first time that high glucose concentration can induce oxidative stress and axonal degeneration in adult sensory neurons, but only if these neurons exhibit an STZ-induced diabetic phenotype. Neurons from normal rats did not exhibit oxidative stress or cell death under high glucose concentrations. High glucose concentration in neurons from diabetic rats triggered elevated ROS levels and adducts of 4-HNE specifically in axons, with the perikarya being unaffected, and this distally directed process of oxidative stress resulted in axonal swelling and axon degeneration. This neurodegenerative process may have been triggered or exacerbated by impaired anti-oxidant defenses, as evidenced by the diminished expression of MnSOD in axons. However, these
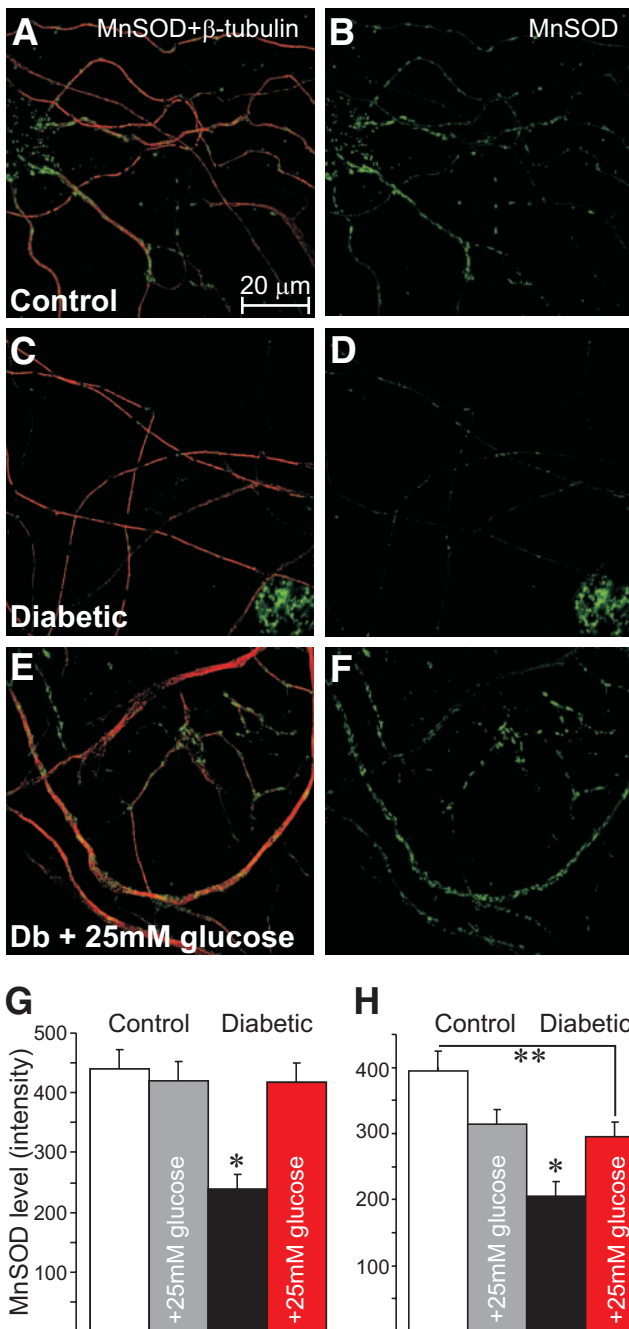
**FIG. 9. Effect of STZ-diabetes on expression of MnSOD in axons of cultured sensory neurons. Lumbar dorsal root ganglion sensory neurons were isolated from age-matched normal or 5-month STZ-diabetic rats and cultured with 10 mmol/l (white or black bars) or 25 mmol/l (gray or red bars) glucose for 1 or 3 days. *A–F*: Cells were fixed and immunofluorescently costained for β-tubulin III (red; neuron specific) (panels *A*, *C*, and *E* show double stain) and MnSOD (green) (panels *B*, *D*, and *F* show single stain). Charts show 1 day (*G*) and 3 days (*H*) of MnSOD expression in axons assessed by fluorescence intensity at ×100 on a confocal microscope. Values are the means ± SE, *n* = 65–94 axons. \*$P < 0.05$ vs. other groups; \*\*$P < 0.05$. (A high-quality digital representation of this figure is available in the online issue.)**

neurons did not undergo any process of cell death. The appearance and content of the axonal swellings closely resembled dystrophic axons observed in human disease.

Previous studies on cultures of embryonic sensory neurons have shown that high glucose concentration triggers oxidative stress, activation of apoptosis, and death of neurons (4–6). In vitro studies by Russell and col-

leagues (3–5) and Feldman and colleagues (4,6) used glucose concentrations of 45–50 mmol/l and higher and showed, using an array of markers of oxidative stress and apoptosis, that these indexes were enhanced in cultured embryonic neurons. Instead, we found that survival of adult sensory neurons from lumbar dorsal root ganglia of normal or diabetic rats did not change under high glucose concentrations. This supports previous in vitro studies on sensory neuron cultures from adult rats and mice (dissociated and explant), where exposure to a hyperglycemic environment failed to induce neuronal death over 1–8 days (23,24). In addition, embryonic sensory neurons given time to mature in vitro for several weeks also become resistant to the apoptosis-inducing effects of high glucose concentration (25). Differences in culture conditions between embryonic and adult preparations may play a role here, and in particular the presence of nonneurons in the mature and adult cultures may be protective against hyperglycemia.

However, this glucose insensitivity of adult rat sensory neurons with respect to cell survival is in good agreement with in vivo studies on experimentally diabetic rodents (8–10,12,26). In the STZ and BB rat models of type 1 diabetes, there is no loss of dorsal root ganglion neurons until 10–12 months of disease, and by this time there is already extensive distal axon loss (9–11,27). There are clearly a range of effects of STZ-induced diabetes on neuronal survival and fiber loss in rodent models, depending on the rodent and/or strain. Clearly, in rat models, either in vitro or in vivo, neuronal cell loss is not a feature of the pathogenesis that underlies distal axon loss. It should be noted that sensory neurons under diabetic conditions can express markers of apoptosis, e.g., activated caspase-3, but these indexes are dissociated from cell death (8). These varied effects of the diabetic state on neuronal survival in the animal models must be judged with caution given the findings that neuronal cell loss in the human form of the disease is not a major feature of the pathology. Studies on postmortem lumbar dorsal root ganglion and sympathetic ganglia derived from type 2 diabetic patients showed ultrastructure of the neuronal perikarya to be abnormal, with signs of shrinkage and axonal dystrophy; however, there was no evidence of any cell loss (14,15). This lack of clear neuronal cell loss occurred while there was overt distal axonal loss in the epidermis (28–30) and sural nerve (1,2,31) of type 1 and type 2 diabetic patients.

The key finding of the current work is that high glucose concentration induced oxidative stress in the axons of sensory neurons isolated from STZ-diabetic rats. This effect was not caused by osmotic stress, and the presence or absence of insulin in the culture was irrelevant to the development of neurodegeneration. The failure of glucose to enhance such processes in normal neurons clearly reveals the importance of the "STZ-induced diabetic phenotype" of neurons, which we propose provides susceptibility of these neurons to glucose-induced metabolic stress. Whether such neurons have a metabolic memory related to previous high glucose concentration–related stress is impossible to ascertain at this juncture. A more profitable line of reasoning relates to growth factor starvation and alterations in the phenotype of the neuron. During 3–5 months of STZ-diabetes, the loss of neurotrophic support from insulin, glial cell line–derived neurotrophic factor, nerve growth factor, and neurotrophin-3 has been well described, and it is known that these growth

factors combine to modulate sensory neuron gene expression (32–35). Of particular interest is the ability of insulin and neurotrophin-3 to correct abnormalities in mitochondrial function and calcium homeostasis (17,18,36). Therefore, in the cultures from diabetic rats studied herein, it is feasible that the ability to respond to glucose-induced oxidative stress was impaired as a consequence of suboptimal mitochondrial function and dyshomeostasis of $Ca^{2+}$ (37). We believe abnormalities in $Ca^{2+}$ homeostasis leading to raised intracellular $Ca^{2+}$ concentration in neurons in diabetes is important because this key molecular marker of neurodegeneration appears more rapidly in the sensory neurons with the longest axons (36). We know of no other molecular marker of disease that is specifically associated with lumbar dorsal root ganglion sensory neurons with the longest axons. This abnormal $Ca^{2+}$ homeostasis could be attributable to global gene expression changes, including affects on endoplasmic reticulum resident proteins (e.g., SERCA2 [sarcoplasmic reticulum $Ca^{2+}$-ATPase 2]) (38), and in addition diabetes may impair expression of proteins associated with antioxidant defenses (e.g., MnSOD and thioredoxin-interacting protein) (39) and growth factor receptors (e.g., the p75[NTR] receptor) (40). Furthermore, sensitivity of sensory neuron axon outgrowth to extracellular matrix proteins is known to alter under stress, e.g., neurons become more sensitive to fibronectin at the expense of laminin after axonal injury (41). These changes in cellular phenotype could combine to sensitize the cell to high glucose concentration and/or changes in growth factor support.

The axonal swellings observed in diabetic neurons were comprised of accumulation of phosphorylated NFH and mitochondria, as seen in dystrophic axonal swellings in autonomic ganglia and nerve, lumbar dorsal root ganglia, and epidermal nerve fibers of skin in humans with diabetic neuropathy (14,15,42). We hypothesize that axonal swellings are sites of mitochondrial and structural protein (e.g., NFH) accumulation caused by blockade of their axonal transport, and the outcome is a dearth of functioning mitochondria and structural proteins at distal axonal sites. The absence of structural proteins and ATP-generating organelles in the distal axon, where high ATP concentration is required for optimal axonal plasticity in the form of axon sprouting and regeneration (43), will trigger pathological conditions that lead to an absence of efficient axonal plasticity. This process may precede or predispose the axon to degeneration and dissolution, and distal axonal degeneration will follow. A key aspect is that the neurodegenerative process within the epidermis caused by the "STZ-induced diabetic state" will not be repaired through normal regenerative processes because these repair functions will also be targeted. The diabetic state as envisaged would include toxic effects of high glucose concentration in addition to abnormalities in neurotrophic support.

We believe these degenerative processes proceed more vigorously in the axon than the perikaryal region of sensory neurons, and this explains the distal dying back nature of diabetic sensory polyneuropathy. The axonal environment during axon sprouting and regeneration would have a very high ATP demand; in fact, 50% of all ATP synthesized is required for growth cone motility during axon sprouting and regeneration (43). Also, ROS scavenging systems, primarily MnSOD, may not be as efficient in the axon because of reduced expression. Figure 9 shows that sensory neurons with a STZ-diabetic phenotype can mount an MnSOD-based antioxidant defense in axons in response to high glucose; however, by 3 days in vitro, the upregulation of MnSOD expression shows signs of failing and may contribute to enhanced oxidative stress and associated aberrant axon structure (Fig. 9*H*). These events may combine to place an additional load on mitochondrial bioenergetics not seen in the perikarya and sensitize the physiology of the organelle to elevations in $Ca^{2+}$ and high glucose concentration.

## REFERENCES

1. Malik RA, Tesfaye S, Newrick PG, Walker D, Rajbhandari SM, Siddique I, Sharma AK, Boulton AJ, King RH, Thomas PK, Ward JD. Sural nerve pathology in diabetic patients with minimal but progressive neuropathy. Diabetologia 2005;48:578–585
2. Yagihashi S. Pathology and pathogenetic mechanisms of diabetic neuropathy. Diabetes Metab Rev 1995;11:193–225
3. Vincent AM, Brownlee M, Russell JW. Oxidative stress and programmed cell death in diabetic neuropathy. Ann N Y Acad Sci 2002;959:368–383
4. Russell JW, Golovoy D, Vincent AM, Mahendru P, Olzmann JA, Mentzer A, Feldman EL. High glucose-induced oxidative stress and mitochondrial dysfunction in neurons. FASEB J 2002;16:1738–1748
5. Vincent AM, Olzmann JA, Brownlee M, Sivitz WI, Russell JW. Uncoupling proteins prevent glucose-induced neuronal oxidative stress and programmed cell death. Diabetes 2004;53:726–734
6. Vincent AM, McLean LL, Backus C, Feldman EL. Short-term hyperglycemia produces oxidative damage and apoptosis in neurons. FASEB J 2005;19:638–640
7. Kennedy JM, Zochodne DW. Experimental diabetic neuropathy with spontaneous recovery: is there irreparable damage? Diabetes 2005;54:830–837
8. Cheng C, Zochodne DW. Sensory neurons with activated caspase-3 survive long-term experimental diabetes. Diabetes 2003;52:2363–2371
9. Zochodne DW, Verge VM, Cheng C, Sun H, Johnston J. Does diabetes target ganglion neurones? Progressive sensory neurone involvement in long-term experimental diabetes. Brain 2001;124:2319–2334
10. Kamiya H, Zhangm W, Sima AA. Apoptotic stress is counterbalanced by survival elements preventing programmed cell death of dorsal root ganglions in subacute type 1 diabetic BB/Wor rats. Diabetes 2005;54:3288–3295
11. Kamiya H, Zhang W, Sima AA. Degeneration of the Golgi and neuronal loss in dorsal root ganglia in diabetic BioBreeding/Worcester rats. Diabetologia 2006;49:2763–2774
12. Jiang Y, Zhang JS, Jakobsen J. Differential effect of p75 neurotrophin receptor on expression of pro-apoptotic proteins c-jun, p38 and caspase-3 in dorsal root ganglion cells after axotomy in experimental diabetes. Neuroscience 2005;132:1083–1092
13. Kalichman MW, Powell HC, Mizisin AP. Reactive, degenerative, and proliferative Schwann cell responses in experimental galactose and human diabetic neuropathy. Acta Neuropathol 1998;95:47–56
14. Schmidt RE, Dorsey D, Parvin CA, Beaudet LN, Plurad SB, Roth KA. Dystrophic axonal swellings develop as a function of age and diabetes in human dorsal root ganglia. J Neuropathol Exp Neurol 1997;56:1028–1043

15. Schmidt RE, Beaudet LN, Plurad SB, Dorsey DA. Axonal cytoskeletal pathology in aged and diabetic human sympathetic autonomic ganglia. Brain Res 1997;769:375–383
16. Lindsay RM. Nerve growth factors (NGF, BDNF) enhance axonal regeneration but are not required for survival of adult sensory neurons. J Neurosci 1988;8:2394–2405
17. Huang TJ, Price SA, Chilton L, Calcutt NA, Tomlinson DR, Verkhratsky A, Fernyhough P. Insulin prevents depolarization of the mitochondrial inner membrane in sensory neurons of type 1 diabetic rats in the presence of sustained hyperglycemia. Diabetes 2003;52:2129–2136
18. Huang TJ, Sayers NM, Verkhratsky A, Fernyhough P. Neurotrophin-3 prevents mitochondrial dysfunction in sensory neurons of streptozotocin-diabetic rats. Exp Neurol 2005;194:279–283
19. Huang TJ, Verkhratsky A, Fernyhough P. Insulin enhances mitochondrial inner membrane potential and increases ATP levels through phosphoinositide 3-kinase in adult sensory neurons. Mol Cell Neurosci 2005;28:42–54
20. Fernyhough P, Smith DR, Schapansky J, Van Der Ploeg R, Gardiner NJ, Tweed CW, Kontos A, Freeman L, Purves-Tyson TD, Glazner GW. Activation of nuclear factor-kappaB via endogenous tumor necrosis factor alpha regulates survival of axotomized adult sensory neurons. J Neurosci 2005;25:1682–1690
21. Mattson MP, Barger SW, Begley JG, Mark RJ. Calcium, free radicals, and excitotoxic neuronal death in primary cell culture. Methods Cell Biol 1995;46:187–216
22. Gardiner NJ, Fernyhough P, Tomlinson DR, Mayer U, von der Mark H, Streuli CH. Alpha7 integrin mediates neurite outgrowth of distinct populations of adult sensory neurons. Mol Cell Neurosci 2005;28:229–240
23. Gumy LF, Bampton ET, Tolkovsky AM. Hyperglycaemia inhibits Schwann cell proliferation and migration and restricts regeneration of axons and Schwann cells from adult murine DRG. Mol Cell Neurosci 2008;37:298–311
24. Purves T, Middlemas A, Agthong S, Jude EB, Boulton AJ, Fernyhough P, Tomlinson DR. A role for mitogen-activated protein kinases in the etiology of diabetic neuropathy. FASEB J 2001;15:2508–2514
25. Yu C, Rouen S, Dobrowsky RT. Hyperglycemia and downregulation of caveolin-1 enhance neuregulin-induced demyelination. Glia 2008;56:877–887
26. Sango K, Horie H, Saito H, Ajiki K, Tokashiki A, Takeshita K, Ishigatsubo Y, Kawano H, Ishikawa Y. Diabetes is not a potent inducer of neuronal cell death in mouse sensory ganglia, but it enhances neurite regeneration in vitro. Life Sci 2002;71:2351–2368
27. Bianchi R, Buyukakilli B, Brines M, Savino C, Cavaletti G, Oggioni N, Lauria G, Borgna M, Lombardi R, Cimen B, Comelekoglu U, Kanik A, Tataroglu C, Cerami A, Ghezzi P. Erythropoietin both protects from and reverses experimental diabetic neuropathy. Proc Natl Acad Sci U S A 2004;101:823–828
28. Ebenezer GJ, McArthur JC, Thomas D, Murinson B, Hauer P, Polydefkis M, Griffin JW. Denervation of skin in neuropathies: the sequence of axonal and Schwann cell changes in skin biopsies. Brain 2007;130:2703–2714
29. Kennedy WR, Wendelschafer-Crabb G, Johnson T. Quantitation of epidermal nerves in diabetic neuropathy. Neurology 1996;47:1042–1048
30. Polydefkis M, Hauer P, Sheth S, Sirdofsky M, Griffin JW, McArthur JC. The time course of epidermal nerve fibre regeneration: studies in normal controls and in people with diabetes, with and without neuropathy. Brain 2004;127:1606–1615
31. Sima AA, Kamiya H. Diabetic neuropathy differs in type 1 and type 2 diabetes. Ann N Y Acad Sci 2006;1084:235–249
32. Akkina SK, Patterson CL, Wright DE. GDNF rescues nonpeptidergic unmyelinated primary afferents in streptozotocin-treated diabetic mice. Exp Neurol 2001;167:173–182
33. Calcutt NA, Jolivalt CG, Fernyhough P. Growth factors as therapeutics for diabetic neuropathy. Curr Drug Targets 2008;9:47–59
34. Christianson JA, Riekhof JT, Wright DE. Restorative effects of neurotrophin treatment on diabetes-induced cutaneous axon loss in mice. Exp Neurol 2003;179:188–199
35. Toth C, Brussee V, Zochodne DW. Remote neurotrophic support of epidermal nerve fibres in experimental diabetes. Diabetologia 2006;49:1081–1088
36. Huang TJ, Sayers NM, Fernyhough P, Verkhratsky A. Diabetes-induced alterations in calcium homeostasis in sensory neurones of streptozotocin-diabetic rats are restricted to lumbar ganglia and are prevented by neurotrophin-3. Diabetologia 2002;45:560–570
37. Verkhratsky A, Fernyhough P. Mitochondrial malfunction and Ca2+ dyshomeostasis drive neuronal pathology in diabetes. Cell Calcium 2008;44:112–122
38. Vetter R, Rehfeld U, Reissfelder C, Weiss W, Wagner KD, Gunther J, Hammes A, Tschope C, Dillmann W, Paul M. Transgenic overexpression of the sarcoplasmic reticulum Ca2+ATPase improves reticular Ca2+ handling in normal and diabetic rat hearts. FASEB J 2002;16:1657–1659
39. Price SA, Gardiner NJ, Duran-Jimenez B, Zeef LA, Obrosova IG, Tomlinson DR. Thioredoxin interacting protein is increased in sensory neurons in experimental diabetes. Brain Res 2006;1116:206–214
40. Delcroix JD, Michael GJ, Priestley JV, Tomlinson DR, Fernyhough P. Effect of nerve growth factor treatment on p75NTR gene expression in lumbar dorsal root ganglia of streptozocin-induced diabetic rats. Diabetes 1998;47:1779–1785
41. Gardiner NJ, Moffatt S, Fernyhough P, Humphries MJ, Streuli CH, Tomlinson DR. Preconditioning injury-induced neurite outgrowth of adult rat sensory neurons on fibronectin is mediated by mobilisation of axonal alpha5 integrin. Mol Cell Neurosci 2007;35:249–260
42. Lauria G, Morbin M, Lombardi R, Borgna M, Mazzoleni G, Sghirlanzoni A, Pareyson D. Axonal swellings predict the degeneration of epidermal nerve fibers in painful neuropathies. Neurology 2003;61:631–636
43. Bernstein BW, Bamburg JR. Actin-ATP hydrolysis is a major energy drain for neurons. J Neurosci 2003;23:1–6